

# UC Davis

## UC Davis Previously Published Works

### Title

Collagen-binding nanoparticles for extracellular anti-inflammatory peptide delivery decrease platelet activation, promote endothelial migration, and suppress inflammation

### Permalink

<https://escholarship.org/uc/item/18h3m652>

### Authors

McMasters, James  
Panitch, Alyssa

### Publication Date

2017-02-01

### DOI

10.1016/j.actbio.2016.11.023

Peer reviewed



Published in final edited form as:

*Acta Biomater.* 2017 February ; 49: 78–88. doi:10.1016/j.actbio.2016.11.023.

## Collagen-Binding Nanoparticles for Extracellular Anti-Inflammatory Peptide Delivery Decrease Platelet Activation, Promote Endothelial Migration, and Suppress Inflammation

James McMasters<sup>a,1</sup> and Alyssa Panitch<sup>a,1,\*</sup>

<sup>a</sup>Weldon School of Biomedical Engineering, Purdue University, 206 South Martin Jischke Drive, West Lafayette, IN 47906

### Abstract

Peripheral artery disease is an atherosclerotic stenosis in the peripheral vasculature that is typically treated via percutaneous transluminal angioplasty. Deployment of the angioplasty balloon damages the endothelial layer, exposing the underlying collagen and allowing for the binding and activation of circulating platelets which initiate an inflammatory cascade leading to eventual restenosis. Here, we report on collagen-binding sulfated poly(N-isopropylacrylamide) nanoparticles that are able to target to the denuded endothelium. Once bound, these nanoparticles present a barrier that reduces cellular and platelet adhesion to the collagenous surface by 67% in whole blood and 59% in platelet-rich plasma under biologically relevant shear rates. *In vitro* studies indicate that the collagen-binding nanoparticles are able to load and release therapeutic quantities of anti-inflammatory peptides, with the particles reducing inflammation in endothelial and smooth muscle cells by 30% and 40% respectively. Once bound to collagen, the nanoparticles increased endothelial migration while avoiding uptake by smooth muscle cells, indicating that they may promote regeneration of the damaged endothelium while remaining anchored to the collagenous matrix and locally releasing anti-inflammatory peptides into the injured area. Combined, these collagen-binding nanoparticles have the potential to reduce inflammation, and the subsequent restenosis, while simultaneously promoting endothelial regeneration following balloon angioplasty.

### Graphical abstract

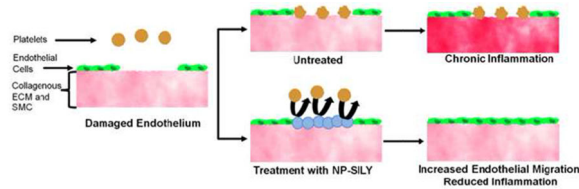
\*Corresponding author: Phone: 1 (530) 754-3222 Fax: 1 (530) 754-5739, apanitch@ucdavis.edu.

<sup>1</sup>Present address: Department of Biomedical Engineering, University of California, Davis, One Shields Avenue, Davis, CA 95616

**Publisher's Disclaimer:** This is a PDF file of an unedited manuscript that has been accepted for publication. As a service to our customers we are providing this early version of the manuscript. The manuscript will undergo copyediting, typesetting, and review of the resulting proof before it is published in its final citable form. Please note that during the production process errors may be discovered which could affect the content, and all legal disclaimers that apply to the journal pertain.

#### Disclosures

Moerae Matrix, Inc. has a worldwide exclusive license to the MK2 inhibitor peptide. Alyssa Panitch owns greater than 5% of Moerae Matrix, Inc.



## Keywords

N-isopropylacrylamide; Thermosensitive polymer; Collagen; Platelet; Anti-Inflammatory Peptides

## 1. Introduction

Peripheral artery disease (PAD) is characterized by an atherosclerotic stenosis within the peripheral vasculature. Despite improved screening effectiveness, PAD still affects over 25% of adults over 55, and is even more prevalent in patients with cardiovascular risk factors such as smoking and hypertension [1-6]. Additionally, PAD is associated with increased risk of other cardiovascular diseases, making the development of an effective long-term treatment of paramount importance to the large population that lives with this disease [7, 8].

The current standard of treatment for severe PAD is percutaneous transluminal angioplasty, sometimes coupled with stent deployment to hold open the widened vessel. A major drawback of angioplasty is that balloon deployment damages the vessel wall, thus exposing the underlying collagenous matrix [9]. Circulating platelets can then bind to the sub-endothelial collagen and become activated, releasing a host of pro-inflammatory factors including epidermal growth factor (EGF), IL-1 $\beta$ , and platelet derived growth factor (PDGF) [10-12]. Smooth muscle cells (SMC) exposed to these factors then become activated and proliferative, resulting in intimal hyperplasia and eventual restenosis, or narrowing of the vessel wall [13-17]. This process is further accelerated by pro-inflammatory cytokines released by the activated SMC, including tumor necrosis factor- $\alpha$  (TNF- $\alpha$ ), interleukin-1 $\beta$  (IL-1 $\beta$ ), interleukin-8 (IL-8) and interleukin-6 (IL-6) [18-20]. The development of restenosis can lead to peripheral limb ischemia, with treatment often necessitating a second angioplasty procedure to open the re-occluded vessel.

Rather than treating restenosis by attenuating the inflammatory cascade, current surgical methods utilize drug-loaded stents that release cytostatic compounds such as paclitaxel and sirolimus to combat the inflammation-induced cellular proliferation. While they are effective at inhibiting intimal hyperplasia [21-24], these compounds are untargeted and thus inhibit the proliferation of local endothelial cells along with the SMC [22, 23]. This results in incomplete healing of the treated area, leaving the stent and collagenous tissue chronically exposed and leading to long-term complications such as late stent thrombosis [25, 26]. Additionally, stents deployed in the peripheral vasculature have a high fracture rate due to the higher crushing and torsional forces they experience [27-29]. These issues make drug-eluting stents a sub-optimal method to prevent restenosis following angioplasty. Thus there exists a need for an improved treatment system that can be deployed during angioplasty to attenuate the subsequent inflammation and promote healing of the damaged vessel.

We have previously reported on a cell penetrating anti-inflammatory peptide (KAFAKLAARLYRKALARQLGVAA abbreviated KAFAK) that can reduce the expression of pro-inflammatory cytokines, by inhibiting mitogen-activated protein kinase activated protein kinase 2 (MK2) [30]. MK2 increases the production of pro-inflammatory cytokines, such as TNF- $\alpha$  and IL-6, regulating inflammation in several diseases, including atherosclerosis [31-35]. While KAFAK has been effective at reducing pro-inflammatory cytokine levels, poor bioavailability in the presence of serum proteases limits its efficacy [36-38]. Therefore it is desirable to use a delivery system that can protect the peptide from proteolytic degradation while providing a sustained release profile *in vivo*, thereby increasing KAFAK's therapeutic efficacy while providing local delivery to the injured area [38-40].

Poly(N-isopropylacrylamide) (pNIPAM) is a thermosensitive polymer that has been extensively studied in biological applications as it exhibits a physiologically relevant lower critical solution temperature (LCST) around 33°C [41-47]. At temperatures below the LCST, crosslinked pNIPAM microgels are in a swollen hydrophilic state, allowing for the loading of water-soluble therapeutics via passive diffusion. Above the LCST, the particle then undergoes hydrophobic collapse, entrapping the loaded drug and allowing for a controlled diffusion out of the particle [38, 40, 47]. In addition, pNIPAM is readily copolymerized with other monomers such as acrylic acid (AAC) to provide easily modified functional groups. *Bartlett et al.* reported that the addition of the sulfated monomer 2-acrylamido-2-methyl-1-propanesulfonic acid (AMPS) to the NIPAM backbone results in a charged nanoparticle that offers increased loading of cationic therapeutics via electrostatic attraction [38, 40]. Additionally, loading the peptide into the nanoparticle provided protection from proteolytic degradation while reducing osteoarthritic inflammation [48]. However these particles were untargeted, allowing them to diffuse away from the site of injury, thus limiting their potential for targeted release. This limitation can be overcome by modifying the delivery system with a targeting ligand that is specific to the damaged area. A particle successfully targeted to the balloon-injured vessel would be able to bind to the damaged area, and remain bound in the presence of blood flow, while locally releasing anti-inflammatory peptides to attenuate the inflammatory cascade.

We have reported on a collagen I binding peptide (RRANAALKAGELYKSILYGC abbreviated SILY) that has been shown to bind to type 1 collagen and prevent platelet adhesion and activation when attached to a dermatan sulfate backbone, while reducing intimal hyperplasia and platelet adhesion *in vivo* [49, 50]. Additionally, pNIPAM nanoparticles modified with SILY have been shown to bind to collagen and prevent platelet activation while still providing a sustained release of their loaded peptide [51]. However, these studies were conducted in a static environment and did not investigate their efficacy *in vitro*. Here, we show that SILY-modified pNIPAM nanoparticles are effective at inhibiting platelet binding under biologically relevant flow conditions, and are capable of binding to SMC-elaborated collagen *in vitro*. Additionally, KAFAK-loaded nanoparticles effectively inhibit inflammation in endothelial cells (EC) and SMC while inhibiting platelet adhesion and demonstrating minimal cytotoxicity.

## 2. Materials and Methods

### 2.1 Nanoparticle Synthesis

pNIPAm containing 5 mol% 2-acrylamido-2-methyl-1-propanesulfonic acid (AMPS) and 1 mol% Acrylic Acid (AAc) were synthesized in a precipitation polymerization reaction as described previously [44, 51]. Briefly, 794.1 mg of NIPAm (Thermo Fisher Scientific), 28.5 mg of N,N'-methylenebisacrylamide (MBA, Sigma-Aldrich), and 76.5 mg of AMPS (Sigma-Aldrich) were added to 70 °C MilliQ water (18.2 MΩ-cm resistivity, Millipore) that had been refluxed under nitrogen for 30 minutes. 5 μL of AAc (99.5%, Thermo Fisher Scientific) and 164 μL of sodium dodecyl sulfate (SDS, 10% w/v, Sigma-Aldrich) were added to the solution, and polymerization was initiated by the addition of 33.7 mg of potassium persulfate (Sigma-Aldrich). For fluorescent nanoparticle synthesis, 1 mol% fluorescein o-acrylate was pre-dissolved in 3% DMSO and then added to the shell polymer mixture and allowed to equilibrate for 30 minutes before the initiation of polymerization. After 5 hours, the reaction was cooled to room temperature and then dialyzed against MilliQ water for 7 days using a 15,000 MWCO dialysis membrane (Spectra-Por). Following dialysis, the purified poly(NIPAm-MBA-AMPS-AAc) nanoparticles were lyophilized and stored at room temperature.

### 2.2 Fabrication of Peptide-Modified Nanoparticles

Collagen binding nanoparticles were fabricated by using 1-Ethyl-3-(3-dimethylaminopropyl)carbodiimide hydrochloride (EDC) and the heterobifunctional cross linker N-β-Maleimidopropionic acid hydrazide (BMPH) to crosslink SILY to the carboxylic acid groups of present in the nanoparticle, as described previously with slight modification [51]. First, lyophilized poly(NIPAm-MBA-AMPS-AAc) nanoparticles were activated by dissolving them in a coupling buffer consisting of 0.1 M MES (Sigma-Aldrich), 0.5 M NaCl (Sigma-Aldrich) and 0.4 mg/mL EDC (Thermo Fisher Scientific) at pH 6.0. After 15 minutes, a 1:1 molar equivalent of BMPH (BMPH:AAc) was then added to the solution and allowed to shake at room temperature for 30 minutes. The BMPH conjugated nanoparticles (NP-BMPH) were purified by centrifugation at 18,000g and 25°C for 60 minutes. The pelleted particles were rinsed with MilliQ water and then lyophilized.

For SILY attachment, lyophilized NP-BMPH were then dissolved at 1 mg/mL in 1× PBS, and 1% of the total concentration of the collagen binding peptide RRANAALKAGELYKSILYGC (SILY, 80% purity, Genscript) was added as SILY<sub>biotin</sub> and allowed to shake at room temperature for 45 minutes. The remaining peptide was then added and allowed to react for an additional 120 minutes, to create the SILY-modified nanoparticles (NP-SILY). For particles without SILY<sub>biotin</sub>, the entire amount of SILY was added and allowed to react for 3 hours. The modified particles were purified by centrifugation and resuspension, as described above, and then lyophilized. Non-collagen-binding particles were made using the peptide GVDVDQDGETGC (LFA, 78% purity, Genscript) and following the same protocol.

### 2.3 Cell Culture

Human aortic endothelial cells were grown continually as a monolayer in medium 200 (ThermoFisher Scientific) supplemented with low serum growth supplement (ThermoFisher Scientific) consisting of 1 µg/mL hydrocortisone, 10 ng/mL epidermal growth factor, 3 ng/mL basic fibroblast growth factor, and 10 µg/mL heparin and 2% fetal bovine serum (FBS). Human coronary artery smooth muscle cells (SMC) were grown continually as a monolayer in medium 231 (ThermoFisher Scientific) supplemented with smooth muscle growth supplement (ThermoFisher Scientific) consisting of 2 ng/mL basic fibroblast growth factor, 0.5 ng/mL epidermal growth factor, 5 ng/mL heparin, 2 µg/mL recombinant human insulin-like growth factor, 0.2 µg/mL bovine serum albumin (BSA) and 4.9% FBS. All cells were maintained at 37°C and 5% CO<sub>2</sub> and used between passages 3 and 8.

### 2.4 Endothelial Cell Migration

In order to ensure that NP-SILY does not adversely impact endothelial migration, we used Oris migration kits (Platypus technologies) to measure cellular proliferation after treatment with varying concentrations of modified nanoparticles. For migration on a collagen coated surface, human type I collagen (chronolog) was diluted in isotonic glucose and added to an Oris 96-well plate at a concentration of 10 µg/cm<sup>2</sup> and incubated overnight at 4°C. The collagen solution was removed from the wells and the plate was air dried under UV for 24 hours. The supplied stoppers were inserted into the wells to prevent cellular adhesion to the center of the wells. Endothelial cells were then seeded at 8,000 cells/well and allowed to grow to confluence for 36 hours. The stoppers were then removed, the wells were washed to remove unbound cells, and 100 µL of complete media containing 0, 1, 2, or 4 mg/mL NP-SILY was added to each well. For collagen coated plates, wells were rinsed with media after 30 minutes to remove unbound particles. Cells were then allowed to migrate for 24 hours before being stained with 10 µM CellTracker green (ThermoFisher Scientific) in media for 30 minutes at 37°C. Stained cells were rinsed with PBS and the Oris plate mask was added to isolate the previously blocked area of the plate. Fluorescence was then read on Spectramax M5 plate reader at 492 nm excitation and 517 nm emission. Visualization of endothelial migration was performed with a Zeiss Observer Z1 fluorescent microscope.

### 2.5 NP-SILY Binding to Collagen *In Vitro*

In order to verify NP-SILY's ability to bind to naturally elaborated collagen, we treated proliferative smooth muscle cells with modified nanoparticles. First, SMC were seeded at 50,000 cells/cm<sup>2</sup> on an 8 chambered glass slide (Lab-Tek) and allowed to bind for 24 hours. 200 µL of complete media containing 2, 1, or 0 mg/mL of fluorescent NP-SILY or NP-SILY<sub>biotin</sub> was then added to the chambers and allowed to incubate for 30 minutes or 24 hours before being rinsed 3× with media to remove unbound particles. Fluorescent NP-SILY was used for qualitative images of binding to collagen, while biotinylated NP-SILY provided parallel quantitative assessments of binding.

For studies using biotinylated particles, media was removed and 100 µL of a diluted streptavidin solution (R & D Systems) was added to each well and incubated on a plate shaker at 200 RPM and room temperature for 20 minutes. The plate was rinsed with PBS and 100 µL of a reagent color solution (R & D Systems) was added to each well and

incubated at 200 RPM and room temperature for 20 minutes. Finally, 50  $\mu\text{L}$  of 2N  $\text{H}_2\text{SO}_4$  was added to stop the reaction, and absorbance was read at 450 nm and 540 nm on a SpectraMax M5 plate reader. For visualization of fluorescent collagen-bound NP-SILY, cells were imaged on a Zeiss Observer Z1 fluorescent microscope. Semi-quantitative measurements of amount of bound nanoparticles was determined by using ImageJ to measure the fluorescent area of 3 images of each treatment.

## 2.6 NP-SILY Cytotoxicity

The biocompatibility of SILY-modified nanoparticles was examined with a Vybrant MTT cell proliferation assay (Molecular Probes) according to manufacturer instructions. First, endothelial and smooth muscle cells were seeded in a 96-well tissue culture plate at 30,000 cells/well and 50,000 cells/well respectively and allowed to adhere for 24 hours. The media was removed and fresh media containing varying concentrations of NP-SILY was added to each well and incubated for 24 hours. The media was removed and 100  $\mu\text{L}$  of fresh media was added to each well. The MTT reagent was prepared by dissolving in sterile PBS at a concentration of 5 mg/mL, and 10  $\mu\text{L}$  was added to each well and incubated for 4 hours at 37°C. SDS was then dissolved in 0.01M HCL at a concentration of 100 mg/mL, and 100  $\mu\text{L}$  was added to each well and incubated for 4 hours at 37°C. The absorbance was then read at 570 nm on a Spectramax M5 plate reader.

## 2.7 Peptide Loading of NP-SILY

In order to demonstrate the modified nanoparticles ability to deliver therapeutics in an *in vitro* inflammatory culture system, we loaded the nanoparticles with the anti-inflammatory cell penetrating peptide (American Peptide). To load the nanoparticles SILY-modified nanoparticles and KAFK were co-incubated in MilliQ water at final concentrations of 1 mg/mL and 2 mg/mL respectively and stored at 4°C for 24 hours. Loaded nanoparticles were pelleted via centrifugation, and the supernatant was collected for analysis. A fluoraldehyde o-phthalaldehyde (OPA) assay was performed to determine the amount of KAFK loaded into the nanoparticles. Briefly, 1:10 mixtures of sample and fluoraldehyde OPA were created in opaque 96-well plates (VWR), and the fluorescence was measured at an excitation of 360 nm and emission of 455 nm on a SpectraMax M5 plate reader. Values were compared against a standard to determine the amount of KAFK present in the pre and post-load solution.

## 2.8 Prevention of *In Vitro* Inflammation

Given that platelet activation is an underlying cause of SMC inflammation and proliferation and that mechanical damage from balloon deployment can damage EC and SMC, we investigated the ability of KAFK-loaded NP-SILY to inhibit inflammation in SMC and EC treated with platelet-derived growth factor (PDGF, Peprotech) an inflammatory factor released by activated platelets. SMC were seeded in a 96-well tissue culture plate at a density of 50,000 cells/cm<sup>2</sup> and allowed to adhere for 12 hours before being serum starved by incubation in unsupplemented medium 231 for 24 hours. Cells were then treated with 10 ng/mL PDGF and either KAFK or KAFK-loaded NP-SILY for 24 hours. The media was removed, and the concentration of IL-6 and TNF- $\alpha$  were then measured using an MSD

multi-array human cytokine assay kit (MesoScale Discovery) according to manufacturer instructions.

Briefly, 25  $\mu\text{L}$  of sample was added to a pre-coated high bind plate, covered, and incubated at on a plate shaker at 700 RPM and room temperature for 2 hours. 25  $\mu\text{L}$  of detection antibody solution was then added to each well, and the plate was then covered and incubated at 700 RPM for a further 2 hours. Finally, the plate was washed 3 times with PBS containing 0.05% tween-20. 150  $\mu\text{L}$  of 2 $\times$  read buffer was added to each well, and the plate was read on a QuickPlex SQ 120 plate reader (MesoScale Discovery).

## 2.9 Prevention of Platelet Attachment Under Biologically Relevant Flow Conditions

The ability of NP-SILY to inhibit platelet binding under flow conditions was investigated using collagen-coated IBIDI microchannels to simulate a biological flow environment. First, human monomeric collagen (Chronolog) was diluted in isotonic glucose to and final concentration of 50  $\mu\text{g}/\text{mL}$ . The collagen solution was then pipetted into the channels of an IBIDI  $\mu$ -slide VI<sup>0.1</sup> slide and incubated overnight at 4°C. The coated channels were then washed with 100  $\mu\text{L}$  of PBS, and then blocked for 30 minutes at room temperature with 1% BSA in PBS. The channels were again washed with PBS and varying concentrations of NP-SILY were added to the channels and incubated at 37°C for 30 minutes before being washed a final time.

15 mL of whole blood was collected into citrated vacutainers from healthy volunteers by venipuncture following an approved Purdue IRB protocol and with informed consent. The blood was centrifuged for 20 min at 200G and 25°C and the top layer of platelet-rich plasma (PRP) was collected. PRP and whole blood was then loaded into 3 mL syringes and a syringe pump was used to flow the fluid through the channel at a rate of 2.1 mL/hr, yielding a physiologically relevant shear rate of 375  $\text{s}^{-1}$  [52]. After 30 minutes, the channels were washed with 100  $\mu\text{L}$  of PBS and adherent cells were stained with CellTracker Green using the protocol mentioned previously. Flow channels were imaged on a Zeiss Observer Z1 fluorescent microscope. Three images were taken of each channel, and ImageJ was used to measure total fluorescent area in order to determine the relative binding of cells in each treatment group.

## 2.10 Statistical Analysis

Statistical significance was determined using a one-way ANOVA with a Tukey post-hoc test to compare experimental groups. A significance level of  $\alpha = 0.05$  was used for all comparisons and all data is expressed as mean  $\pm$  standard deviations.

# 3. Results

## 3.1 Nanoparticle Cytotoxicity

In order to remain viable *in vivo* drug delivery platforms, the modified nanoparticles must remain biocompatible at concentrations necessary to release therapeutic levels of KFAK. The MTT assay indicates that there were no significant differences in cellular viability of endothelial (figure 1a) or smooth muscle cells (figure 1b) treated with up to 8 mg/mL of NP-



SILY. This suggests that the nanoparticles can be used to locally deliver therapeutics without inducing a cytotoxic response in the surrounding cells.

### 3.2 Endothelial Migration

Due to the importance of endothelial migration on the healing of the damaged vessel, we investigated whether varying concentrations of NP-SILY impacted endothelial migration (figure 2). As seen in figure 2a, modified nanoparticles have no significant impact on endothelial migration on tissue culture plastic at concentrations below 4 mg/mL; however, higher concentrations of NP-SILY significantly decreased cellular migration. Conversely, an increase in cellular migration on a collagen-coated surface was observed at nanoparticle concentrations above 2 mg/mL (figure 2b).

### 3.3 *In Vitro* Collagen Binding

While the SILY-modified nanoparticles have demonstrated the ability to bind to a collagen-coated surface [51], it is equally important that they have the capability to bind to collagen that is elaborated by the SMC found within the damaged blood vessel. Figure 3 demonstrates NP-SILY's ability to bind to collagen elaborated by human coronary artery smooth muscle cells 24 hours after plating on tissue culture plastic. As seen in the quantitative analysis of NP-SILY<sub>biotin</sub> binding to SMC collagen (figure 3a), biotinylated NP-SILY binds to the collagen matrix following a short 30-minute incubation at the 2 mg/mL concentration, while lower nanoparticle concentrations required a longer incubation to demonstrate the same level of collagen binding. Further, significantly more nanoparticle binding to collagen is seen after 24 hours when the SMCs have had time to secrete additional extracellular collagen. Conversely, nanoparticles modified with the non-collagen-binding LFA peptide demonstrated only a small amount of non-specific binding, even after the longer 24-hour incubation.

Figure 3b shows imaging of fluorescently-labeled nanoparticles bound to the SMC matrix. After 30 minutes of incubation with fluorescent nanoparticles, distinct fiber-like structures are observed on top of the SMC, indicating that NP-SILY successfully binds to the elaborated collagen. After an additional 24 hours of culture, fluorescence can be observed farther away from the SMC, indicating that additional particles bound to the collagen as it was newly elaborated. This is further demonstrated in the semi-quantitative analysis of fluorescent images in figure 3c, which shows that fluorescence is detectable after an initial 30-minute incubation and increases with prolonged incubation, likely due to additional signal from binding to newly elaborated collagen. Finally, after 30 minutes of NP-SILY exposure, fluorescence at 2 mg/mL is significantly higher than fluorescence at 1 mg/mL, indicating increased nanoparticle binding at higher nanoparticle concentrations, likely attributable to larger concentration gradients driving rapid binding to the collagen.

### 3.4 *In Vitro* Inflammatory Inhibition

In order to be a viable treatment for post-angioplasty vessel damage, KAFK must be released at therapeutic concentrations at ~30  $\mu$ M for effective inhibition of inflammation [30]. We investigated KAFK-loaded NP-SILY's ability to inhibit inflammation in endothelial and smooth muscle cells that had been stimulated with PDGF. Figure 4 shows

that the KAFK-loaded nanoparticles were able to reduce inflammation in both cell types, with IL-6 levels decreasing 30% and 40% in endothelial (Figure 4a) and smooth muscle (Figure 4b) cells, respectively. The addition of free-KAFK decreased endothelial inflammation by 80% and decreased SMC inflammation by 16%.

### 3.5 Prevention of Platelet Attachment Under Biologically Relevant Flow Conditions

Beyond providing a platform for the release of therapeutic peptides, the SILY-modified nanoparticles are designed to have dual-therapy potential by preventing platelet activation by binding to the collagenous matrix exposed by the angioplasty procedure. We tested this ability by flowing whole blood or PRP through a collagen-coated microchannel that had been treated with NP-SILY, and then probing for adherent platelets. Figure 5 shows that NP-SILY was effective at preventing binding in both the whole blood and PRP. As shown in figure 5b, the highest tested concentration of NP-SILY reduced binding by 44% in whole blood. Interestingly, binding was further reduced at lower treatment concentrations, with 2 mg/mL doses reducing binding by 53% and 59% in whole blood and PRP respectively. This trend continued at the lowest concentration with 1 mg/mL NP-SILY reducing binding by 67% in whole blood. As can be seen in figure 5a, whole blood yielded larger clusters of bound cells compared to the PRP. This is likely due to the larger overall concentration of cells as well as the presence of red blood cells, which bind to denuded endothelium in the presence of bound platelets and have also been shown to enhance platelet binding [53]. Additionally, binding of platelets and red blood cells could have induced soft clot formation which could account for the large clusters of cells observed in figure 5A I and II

## 4. Discussion

Percutaneous transluminal angioplasty is one of the most common methods used to treat severe PAD. However, deployment of the balloon damages the endothelial layer, exposing the underlying collagenous tissue. Platelet adhesion and activation on this collagen results in the release of proinflammatory factors that lead to SMC activation and eventual intimal hyperplasia and restenosis [9, 13-16]. Here, we demonstrate that a sulfated collagen-binding poly(NIPAm-MBA-AMPS-AAC) nanoparticle, modified with the collagen-binding peptide SILY is able to bind to a collagenous matrix while preventing platelet adhesion and releasing therapeutic concentrations of cell-penetrating anti-inflammatory peptides. Previous work with SILY-modified peptidoglycans indicates that because SILY is derived from the platelet receptor to collagen it is able to competitively inhibit platelet binding to collagen. Additionally, when attached to a large macromolecule, prevention of platelet adhesion occurs through a combination of competitive binding to the collagen as well as steric hindrance provided by the overall size of the bound molecule [49]. A key benefit of preventing the platelet adhesion and subsequent activation is that it attenuates the inflammatory cascade at the initiating event, as opposed to attempting to mitigate the downstream results. Previous studies with collagen binding peptidoglycans have demonstrated that protecting the collagenous layer of the damaged vessel leads to reduced platelet deposition and intimal hyperplasia. These previous studies suggest that our modified nanoparticle has the potential to inhibit the increased SMC migration that is caused by the

activated platelets, possibly resulting in decreased intimal hyperplasia and reduced risk of restenosis [49, 50].

While previous work has demonstrated the biocompatibility of pNIPAM nanoparticles, eliciting low cytotoxicity when taken up by macrophages as well as showing excellent hemocompatibility [38, 54, 55], the surface addition of the collagen-binding peptide SILY has the potential to alter cellular uptake as well as biocompatibility. Additionally, as these modified particles are designed to be administered via porous balloon catheter directly to the damaged vascular environment, which contains migrating endothelial cells as well as proliferating SMC, they must not elicit cytotoxicity if taken up by either cell type. The results of our cytotoxicity analysis indicate that nanoparticles retained biocompatibility with both endothelial and smooth muscle cells at concentrations up to 8 mg/mL, which exceeds the concentration necessary to release therapeutic concentrations of KFAK *in vitro*.

In addition to retaining biocompatibility, the modified nanoparticles must not interfere with the natural regeneration of the endothelial layer, which can occur one week following balloon angioplasty [9]. To this end, we tested endothelial migration on EC seeded on tissue culture plastic as well as a collagen-coated surface. We observed no change in migration of EC seeded on tissue culture plastic at treatment concentrations below 4 mg/mL; however, migration was significantly reduced at higher treatment concentrations. This is likely due to nonspecific binding of the nanoparticles to the tissue culture-treated surface, thus creating a negatively charged surface, which has been shown to reduce endothelial adhesion and migration [56]. Of greater concern is the possibility that nanoparticles bound to a collagen surface may provide a barrier to endothelial migration, resulting in decreased migration rates and, thus, impaired healing of the endothelial layer. Interestingly, collagen-bound nanoparticles increased endothelial migration at treatment concentrations above 1 mg/mL, suggesting that these particles may accelerate endothelial regeneration following angioplasty. A similar increase in endothelial migration was observed in SILY-modified glycosaminoglycans [17], where the increased migration was attributed to the molecules' ability to sequester proliferative growth factors such as fibroblast growth factor-2 (FGF-2). Given the charged nature of the modified nanoparticle, it is possible that a similar mechanism is occurring here; the nanoparticles may act as a reservoir of FGF-2 and other positively charged growth factors, thereby increasing its local concentration and accelerating endothelial migration. Upon visualization of migrating endothelial cells, we observed the presence of migrating cells in the center of the well with markedly fewer cells where the silicone plug was in contact with the surface. This is likely due to damage to the collagen coating following plug removal. This damage would decrease the cells ability to remain adherent to the surface when the collagen layer was disrupted, resulting in the ring of lower cell density that we observed.

While NP-SILY's ability to bind to a collagen-coated surface has been demonstrated previously [51], it is equally important to have the ability to bind to collagen that is organized into a more biologically relevant 3-dimensional matrix. In the body, smooth muscle cells control the elaboration and organization of the collagenous matrix through their expression of integrins and matrix metalloproteinases [13, 57, 58]. To test the ability of SILY-modified nanoparticles to bind to this matrix, we cultured SMC on tissue culture

plastic and observed particle binding after 30 minutes and 24 hours of treatment in both the quantitative NP-SILY<sub>biotin</sub> assay and the semi-quantitative fluorescent image analysis. Interestingly, particle binding in globular forms was observed farther away from the cells after 24 hours (48 hours after seeding) indicating that the particles were able to bind to the collagen as it was secreted by the cells. Additionally, the particles retained their binding ability even after 24 hours in media containing 5% FBS. This indicates that the bound SILY was not proteolytically degraded, nor did the presence and adsorption of serum proteins inhibit SILY's binding affinity. In contrast to the NP binding observed for NP-SILY<sub>biotin</sub>, we did not observe a similar biotin signal for NP-LFA<sub>biotin</sub>, which was as expected for the negative control NP. However, using fluorescence microscopy, we observed fluorescence in SMC that were treated with fluorescent NP-LFA for 24 hours. Interestingly, in contrast to NP-SILY, the fluorescent signal for the NP-LFA was intracellular, with no extracellular fluorescence observed. This indicates that the NP-LFA particles were internalized by the SMC, as the streptavidin assay used with the biotinylated NP-LFA particles yielded minimal signal due to the inability of streptavidin to penetrate the cell membrane and bind to the internalized biotinylated particles. Importantly, this demonstrates that conjugation of SILY and subsequent binding of the NP-SILY to collagen prevented cellular uptake of the nanoparticles, meaning that they would remain in the extracellular matrix where they would be able to release therapeutic peptides into the inflamed environment.

Once bound to collagen, the NP-SILY is designed to competitively inhibit collagen-induced platelet adhesion and activation. While this has been demonstrated in a static collagen-coated plate [51], the presence of a flow-induced shear force has the potential to cause delamination of the collagen-bound nanoparticles and with it their platelet inhibition. Whole blood flow experiments, at physiologically relevant flow rates, demonstrated an inversely proportional dose-dependent decrease in cell binding between 44% and 67%. Similarly, flow experiments with PRP at 2 mg/mL yielded a 59% reduction in bound platelets. It should be noted that the measurements taken in whole blood included total binding of multiple cell types and thus were not specific to platelets. These results are consistent with our previous work that shows that platelet inhibition was highest at 2 mg/mL, suggesting that high concentrations of bound particles may increase cellular interaction possibly by changing the charge properties of the surface or through a surface roughening effect which could disrupt surface flow and increase cellular interaction. This will need to be carefully evaluated in vivo in future studies. When taken together with the measured reduction in platelet binding, this data indicates that, at appropriate concentrations, the barrier formed by the NP-SILY is not only effective at reducing platelet adhesion, but provides a general protective layer that prevents other cellular interactions with the collagen surface. While specific measurements of nanoparticle binding under flow were not obtained, nanoparticle detachment is not expected to present a problem given the numerous SILY peptides per nanoparticle. Additionally, the optimal time to administer the nanoparticles would be during the angioplasty procedure, before any platelet adhesion has occurred. This could most easily be accomplished through the use of a porous angioplasty balloon, which have been used to deliver therapeutics such as paclitaxel, thrombolytic agents [59], and nanoparticles [60]. During administration the balloon is in contact with the vessel wall, resulting in minimal flow which enables optimal nanoparticle binding to the denuded surface in a static

environment. While the differences in *in vitro* and *in vivo* binding time are a limitation of this study, with the nanoparticles having less time to bind when administered through a balloon, the peptide's high binding affinity combined with the force generated by the balloon against the vessel wall leads us to expect that the nanoparticles will be able to coat the vessel prior to balloon withdrawal.

Once bound, the nanoparticles are designed to act as a platform for the controlled release of anti-inflammatory cell-penetrating peptides. The local release of these peptides into the damaged vessel would attenuate inflammation induced by mechanical damage caused by balloon deployment. Combined with the reduction in platelet binding and activation these nanoparticles can act as a dual therapy platform, inhibiting platelet binding-induced damage while releasing therapeutics to treat the underlying inflammatory state. We tested the ability of these particles to load and release the peptide KAFK in the presence of inflamed smooth muscle and endothelial cells. In these tests, the particles successfully reduced inflammation measured by the production of IL-6. Treatment with KAFK-loaded NP-SILY effectively reduced IL-6 levels by 30% in inflamed endothelial cells, while free KAFK reduced inflammation by 80%. It appears that the KAFK-loaded NP-SILY treatment was less effective than free-KAFK, suggesting that the delivered KAFK dose could be below the therapeutic range specific for endothelial cells; this indicates that cell-specific dose optimization may be required. Alternatively, since the EC media contained less serum than SMC media (2% vs. 5%) creating a less proteolytic environment, it is possible that decreased free-KAFK degradation led to a higher therapeutic response. Given that SMC are a large component of the inflammatory cascade, and that their migration can directly lead to restenosis, it is of paramount importance that these particles effectively treat inflamed SMC. To this end, treatment with KAFK-loaded particles reduced IL-6 production 40%, back to basal levels after 24 hours. Previous *in vitro* studies using these peptides have shown a 30  $\mu$ M dose inhibits inflammation in mesothelial cells to a similar degree to what we observed in our smooth muscle cells [30]. *In vivo* studies have also demonstrated significant reductions in inflammation following topical administrations of low doses of similar anti-inflammatory MK2 inhibitor peptides [61, 62]. Because of this, we expect similar results when we proceed to *in vivo* studies, due to the particles ability to both inhibit platelet adhesion and activation and reduce inflammation [51]. While there is some concern that *in vivo* delivery would result in rapid removal of KAFK from the damaged area, the use of a cell-penetrating peptide helps to mitigate this concern. Previous *in vivo* studies indicate that the presence of a cell-penetrating domain facilitates rapid and active uptake into cells, suggesting that it should be able to exert its biological activity prior to being removed from the damaged area[30, 61-63].

## 5. Conclusion

We have developed a biocompatible dual therapy collagen-binding poly(NIPAm-MBA-AMPS-AAc) nanoparticle that is able to prevent platelet binding and activation while releasing therapeutic doses of the anti-inflammatory cell-penetrating peptide KAFK. *In vitro* inflammatory models show that treatment with KAFK-loaded nanoparticles significantly reduced pro-inflammatory cytokine levels in both inflamed SMC and endothelial cells. Building on our previous work that demonstrated a greater than 60%

inhibition in collagen-induced platelet activation [51] nanoparticles at 1mg/mL reduced cellular adhesion (red blood cells, leukocytes, and platelets) and platelet adhesion to a collagen surface by 67% and 59% respectively under biologically relevant flow conditions, indicating their potential to attenuate the inflammatory cascade initiated by platelet adhesion and activation. Finally, NP-SILY is able to bind to the collagenous matrix elaborated by SMC, avoiding uptake of the nanoparticles by proliferating SMC and allowing local the release of KFAK into the damaged area. Combined, these properties indicate NP-SILY's potential as a dual therapy platform that is able to inhibit restenosis of a treated vessel by attenuating the platelet activation-induced inflammatory cascade while simultaneously delivering therapeutic peptides to inhibit the inflammatory response of cells damaged by balloon deployment. Future work will focus on characterizing the particles potential for site-specific delivery via porous catheter balloon, as well as its ability to bind to the denuded endothelium of an explanted porcine carotid artery. Additionally, *in vivo* studies will need to be conducted to confirm that KFAK-loaded NP-SILY is a viable option for the inhibition of restenosis following balloon angioplasty, specifically looking for a reduction in intimal hyperplasia and a decrease in platelet and macrophage deposition.

## Acknowledgments

Funding: This work was supported by the National Institutes of Health [HL106792]. Funding sources had no involvement in study design, collection and analysis of data, or decision to publish.

## References

- [1]. Cacoub P, Cambou JP, Kownator S, Belliard JP, Beregi JP, Branchereau A, Carpentier P, Léger P, Luzy F, Maïza D. Prevalence of peripheral arterial disease in high-risk patients using ankle-brachial index in general practice: a cross-sectional study. *International journal of clinical practice*. 2009; 63(1):63–70. [PubMed: 19125994]
- [2]. Cimminiello C, Borghi C, Kownator S, Wautrecht JC, Carvounis CP, Kranendonk SE, Kindler B, Mangrella M, P.S. Investigators. Prevalence of peripheral arterial disease in patients at non-high cardiovascular risk. Rationale and design of the PANDORA study. *BMC Cardiovasc Disord*. 2010; 10:35. [PubMed: 20687927]
- [3]. Criqui MH, Fronek A, Barrett-Connor E, Klauber MR, Gabriel S, Goodman D. The prevalence of peripheral arterial disease in a defined population. *Circulation*. 1985; 71(3):510–5. [PubMed: 3156006]
- [4]. Diehm C, Lange S, Darius H, Pittrow D, von Stritzky B, Tepohl G, Haberl RL, Allenberg JR, Dasch B, Trampisch HJ. Association of low ankle brachial index with high mortality in primary care. *Eur Heart J*. 2006; 27(14):1743–9. [PubMed: 16782720]
- [5]. Hirsch AT, Criqui MH, Treat-Jacobson D, Regensteiner JG, Creager MA, Olin JW, Krook SH, Hunninghake DB, Comerota AJ, Walsh ME, McDermott MM, Hiatt WR. Peripheral arterial disease detection, awareness, and treatment in primary care. *JAMA*. 2001; 286(11):1317–24. [PubMed: 11560536]
- [6]. Selvin E, Erlinger TP. Prevalence of and risk factors for peripheral arterial disease in the United States: results from the National Health and Nutrition Examination Survey, 1999–2000. *Circulation*. 2004; 110(6):738–43. [PubMed: 15262830]
- [7]. Aronow WS, Ahmed MI, Ekundayo OJ, Allman RM, Ahmed A. A propensity-matched study of the association of peripheral arterial disease with cardiovascular outcomes in community-dwelling older adults. *Am J Cardiol*. 2009; 103(1):130–5. [PubMed: 19101243]
- [8]. Dalmia S, Pathak R, Callum K. Five-year duplex follow up of femoropopliteal percutaneous transluminal angioplasty. 2005

- [9]. Steele PM, Chesebro JH, Stanson AW, Holmes DR Jr, Dewanjee MK, Badimon L, Fuster V. Balloon angioplasty. Natural history of the pathophysiological response to injury in a pig model. *Circ Res*. 1985; 57(1):105–12. [PubMed: 3159504]
- [10]. Kaplan KL, Broekman MJ, Chernoff A, Lesznik GR, Drillings M. Platelet alpha-granule proteins: studies on release and subcellular localization. *Blood*. 1979; 53(4):604–18. [PubMed: 426909]
- [11]. Lindemann S, Tolley ND, Dixon DA, McIntyre TM, Prescott SM, Zimmerman GA, Weyrich AS. Activated platelets mediate inflammatory signaling by regulated interleukin 1beta synthesis. *J Cell Biol*. 2001; 154(3):485–90. [PubMed: 11489912]
- [12]. Eppley BL, Woodell JE, Higgins J. Platelet quantification and growth factor analysis from platelet-rich plasma: implications for wound healing. *Plast Reconstr Surg*. 2004; 114(6):1502–8. [PubMed: 15509939]
- [13]. Amento EP, Ehsani N, Palmer H, Libby P. Cytokines and growth factors positively and negatively regulate interstitial collagen gene expression in human vascular smooth muscle cells. *Arterioscler Thromb*. 1991; 11(5):1223–30. [PubMed: 1911708]
- [14]. Hanke H, Strohschneider T, Oberhoff M, Betz E, Karsch KR. Time course of smooth muscle cell proliferation in the intima and media of arteries following experimental angioplasty. *Circ Res*. 1990; 67(3):651–9. [PubMed: 1697794]
- [15]. Karas SP, Gravanis MB, Santoian EC, Robinson KA, Anderberg KA, King SB 3rd. Coronary intimal proliferation after balloon injury and stenting in swine: an animal model of restenosis. *J Am Coll Cardiol*. 1992; 20(2):467–74. [PubMed: 1634687]
- [16]. MacLeod DC, Strauss BH, de Jong M, Escaned J, Umans VA, van Suylen RJ, Verkerk A, de Feyter PJ, Serruys PW. Proliferation and extracellular matrix synthesis of smooth muscle cells cultured from human coronary atherosclerotic and restenotic lesions. *J Am Coll Cardiol*. 1994; 23(1):59–65. [PubMed: 8277096]
- [17]. Perez J, Torres RA, Rocic P, Cismowski MJ, Weber DS, Darley-Usmar VM, Lucchesi PA. PYK2 signaling is required for PDGF-dependent vascular smooth muscle cell proliferation. *American Journal of Physiology-Cell Physiology*. 2011; 301(1):C242–C251. [PubMed: 21451101]
- [18]. Knobloch J, Wahl C, Feldmann M, Jungck D, Strauch J, Stoelben E, Koch A. Resveratrol attenuates the release of inflammatory cytokines from human bronchial smooth muscle cells exposed to lipoteichoic acid in chronic obstructive pulmonary disease. *Basic Clin Pharmacol Toxicol*. 2014; 114(2):202–9. [PubMed: 23981542]
- [19]. Schuliga M, Langenbach S, Xia YC, Qin C, Mok JS, Harris T, Mackay GA, Medcalf RL, Stewart AG. Plasminogen-stimulated inflammatory cytokine production by airway smooth muscle cells is regulated by annexin A2. *Am J Respir Cell Mol Biol*. 2013; 49(5):751–8. [PubMed: 23721211]
- [20]. Yeh J-L, Hsu J-H, Liang J-C, Chen J, Liou S-F. Lercanidipine and labedipinedilol-A attenuate lipopolysaccharide/interferon- $\gamma$ -induced inflammation in rat vascular smooth muscle cells through inhibition of HMGB1 release and MMP-2, 9 activities. *Atherosclerosis*. 2013; 226(2):364–372. [PubMed: 23290263]
- [21]. Daemen J, Wenaweser P, Tsuchida K, Abrecht L, Vaina S, Morger C, Kukreja N, Juni P, Sianos G, Hellige G, van Domburg RT, Hess OM, Boersma E, Meier B, Windecker S, Serruys PW. Early and late coronary stent thrombosis of sirolimus-eluting and paclitaxel-eluting stents in routine clinical practice: data from a large two-institutional cohort study. *Lancet*. 2007; 369(9562):667–78. [PubMed: 17321312]
- [22]. Garcia-Touchard A, Burke SE, Toner JL, Cromack K, Schwartz RS. Zotarolimus-eluting stents reduce experimental coronary artery neointimal hyperplasia after 4 weeks. *Eur Heart J*. 2006; 27(8):988–93. [PubMed: 16449248]
- [23]. Matter CM, Rozenberg I, Jaschko A, Greutert H, Kurz DJ, Wnendt S, Kuttler B, Joch H, Grunenfelder J, Zund G, Tanner FC, Luscher TF. Effects of tacrolimus or sirolimus on proliferation of vascular smooth muscle and endothelial cells. *J Cardiovasc Pharmacol*. 2006; 48(6):286–92. [PubMed: 17204907]
- [24]. Azrin MA, Mitchel JF, Fram DB, Pedersen CA, Cartun RW, Barry JJ, Bow LM, Waters DD, McKay RG. Decreased platelet deposition and smooth muscle cell proliferation after intramural heparin delivery with hydrogel-coated balloons. *Circulation*. 1994; 90(1):433–41. [PubMed: 8026030]

- [25]. Joner M, Finn AV, Farb A, Mont EK, Kolodgie FD, Ladich E, Kutys R, Skorija K, Gold HK, Virmani R. Pathology of drug-eluting stents in humans: delayed healing and late thrombotic risk. *J Am Coll Cardiol*. 2006; 48(1):193–202. [PubMed: 16814667]
- [26]. Joner M, Nakazawa G, Finn AV, Quee SC, Coleman L, Acampado E, Wilson PS, Skorija K, Cheng Q, Xu X, Gold HK, Kolodgie FD, Virmani R. Endothelial cell recovery between comparator polymer-based drug-eluting stents. *J Am Coll Cardiol*. 2008; 52(5):333–42. [PubMed: 18652940]
- [27]. Krajcer Z, Howell MH. Update on endovascular treatment of peripheral vascular disease: new tools, techniques, and indications. *Tex Heart Inst J*. 2000; 27(4):369–85. [PubMed: 11198311]
- [28]. Mongiardo A, Curcio A, Spaccarotella C, Parise S, Indolfi C. Molecular mechanisms of restenosis after percutaneous peripheral angioplasty and approach to endovascular therapy. *Curr Drug Targets Cardiovasc Haematol Disord*. 2004; 4(3):275–87. [PubMed: 15379621]
- [29]. Schillinger M, Sabeti S, Loewe C, Dick P, Amighi J, Mlekusch W, Schlager O, Cejna M, Lammer J, Minar E. Balloon angioplasty versus implantation of nitinol stents in the superficial femoral artery. *N Engl J Med*. 2006; 354(18):1879–88. [PubMed: 16672699]
- [30]. Brugnano JL, Chan BK, Seal BL, Panitch A. Cell-penetrating peptides can confer biological function: regulation of inflammatory cytokines in human monocytes by MK2 inhibitor peptides. *Journal of controlled release*. 2011; 155(2):128–133. [PubMed: 21600941]
- [31]. Hegen M, Gaestel M, Nickerson-Nutter CL, Lin LL, Telliez JB. MAPKAP kinase 2-deficient mice are resistant to collagen-induced arthritis. *J Immunol*. 2006; 177(3):1913–7. [PubMed: 16849504]
- [32]. Culbert AA, Skaper SD, Howlett DR, Evans NA, Facci L, Soden PE, Seymour ZM, Guillot F, Gaestel M, Richardson JC. MAPK-activated protein kinase 2 deficiency in microglia inhibits pro-inflammatory mediator release and resultant neurotoxicity. Relevance to neuroinflammation in a transgenic mouse model of Alzheimer disease. *J Biol Chem*. 2006; 281(33):23658–67. [PubMed: 16774924]
- [33]. Gorska MM, Liang Q, Stafford SJ, Goplen N, Dharajiya N, Guo L, Sur S, Gaestel M, Alam R. MK2 controls the level of negative feedback in the NF-kappaB pathway and is essential for vascular permeability and airway inflammation. *J Exp Med*. 2007; 204(7):1637–52. [PubMed: 17576778]
- [34]. Jagavelu K, Tietge UJ, Gaestel M, Drexler H, Schieffer B, Bavendiek U. Systemic deficiency of the MAP kinase-activated protein kinase 2 reduces atherosclerosis in hypercholesterolemic mice. *Circ Res*. 2007; 101(11):1104–12. [PubMed: 17885219]
- [35]. Kontoyiannis D, Boulougouris G, Manoloukos M, Armaka M, Apostolaki M, Pizarro T, Kotlyarov A, Forster I, Flavell R, Gaestel M, Tsichlis P, Cominelli F, Kollias G. Genetic dissection of the cellular pathways and signaling mechanisms in modeled tumor necrosis factor-induced Crohn's-like inflammatory bowel disease. *J Exp Med*. 2002; 196(12):1563–74. [PubMed: 12486099]
- [36]. Bhaskar Kompella U, Lee VHL. (C) Means to Enhance Penetration: (4) Delivery systems for penetration enhancement of peptide and protein drugs: design considerations. *Advanced Drug Delivery Reviews*. 1992; 8(1):115–162.
- [37]. Bundgaard H. (C) Means to enhance penetration: (1) Prodrugs as a means to improve the delivery of peptide drugs. *Advanced Drug Delivery Reviews*. 1992; 8(1):1–38.
- [38]. Bartlett RL 2nd, Medow MR, Panitch A, Seal B. Hemocompatible poly(NIPAm-MBA-AMPS) colloidal nanoparticles as carriers of anti-inflammatory cell penetrating peptides. *Biomacromolecules*. 2012; 13(4):1204–11. [PubMed: 22452800]
- [39]. Anderson R, Franch A, Castell M, Perez-Cano FJ, Brauer R, Pohlert D, Gajda M, Siskos AP, Katsila T, Tamvakopoulos C, Rauchhaus U, Panzner S, Kinne RW. Liposomal encapsulation enhances and prolongs the anti-inflammatory effects of water-soluble dexamethasone phosphate in experimental adjuvant arthritis. *Arthritis Res Ther*. 2010; 12(4):R147. [PubMed: 20642832]
- [40]. Bartlett RL 2nd, Panitch A. Thermosensitive nanoparticles with pH-triggered degradation and release of anti-inflammatory cell-penetrating peptides. *Biomacromolecules*. 2012; 13(8):2578–84. [PubMed: 22852804]



- [41]. Overstreet DJ, Huynh R, Jarbo K, McLemore RY, Vernon BL. In situ forming, resorbable graft copolymer hydrogels providing controlled drug release. *J Biomed Mater Res A*. 2013; 101(5): 1437–46. [PubMed: 23114985]
- [42]. Overstreet DJ, McLemore RY, Doan BD, Farag A, Vernon BL. Temperature-responsive graft copolymer hydrogels for controlled swelling and drug delivery. *Soft Materials*. 2013; 11(3):294–304.
- [43]. Galperin A, Long TJ, Ratner BD. Degradable, thermo-sensitive poly(N-isopropyl acrylamide)-based scaffolds with controlled porosity for tissue engineering applications. *Biomacromolecules*. 2010; 11(10):2583–92. [PubMed: 20836521]
- [44]. Jones CD, Lyon LA. Dependence of shell thickness on core compression in acrylic acid modified poly (N-isopropylacrylamide) core/shell microgels. *Langmuir*. 2003; 19(11):4544–4547.
- [45]. Saikia A, Aggarwal S, Mandal U. Preparation and controlled drug release characteristics of thermoresponsive PEG/poly (NIPAM-co-AMPS) hydrogels. *International Journal of Polymeric Materials*. 2013; 62(1):39–44.
- [46]. Elaissari, A. *Smart Colloidal Materials*. Springer; 2006. Thermally sensitive colloidal particles: from preparation to biomedical applications; p. 9-14.
- [47]. Schmaljohann D. Thermo- and pH-responsive polymers in drug delivery. *Adv Drug Deliv Rev*. 2006; 58(15):1655–70. [PubMed: 17125884]
- [48]. Bartlett RL 2nd, Sharma S, Panitch A. Cell-penetrating peptides released from thermosensitive nanoparticles suppress pro-inflammatory cytokine response by specifically targeting inflamed cartilage explants. *Nanomedicine : nanotechnology, biology, and medicine*. 2013; 9(3):419–27.
- [49]. Paderi JE, Stuart K, Sturek M, Park K, Panitch A. The inhibition of platelet adhesion and activation on collagen during balloon angioplasty by collagen-binding peptidoglycans. *Biomaterials*. 2011; 32(10):2516–23. [PubMed: 21216002]
- [50]. Scott RA, Paderi JE, Sturek M, Panitch A. Decorin mimic inhibits vascular smooth muscle proliferation and migration. *PloS one*. 2013; 8(11):e82456. [PubMed: 24278482]
- [51]. McMasters J, Panitch A. Prevention of Collagen-Induced Platelet Binding and Activation by Thermosensitive Nanoparticles. *AAPS J*. 2015; 17(5):1117–25. [PubMed: 26070443]
- [52]. Hoeks AP, Samijo SK, Brands PJ, Reneman RS. Noninvasive determination of shear-rate distribution across the arterial lumen. *Hypertension*. 1995; 26(1):26–33. [PubMed: 7607728]
- [53]. Aarts P, Bolhuis PA, Sakariassen KS, Heethaar RM, Sixma JJ. Red blood cell size is important for adherence of blood platelets to artery subendothelium. *Blood*. 1983; 62(1):214–217. [PubMed: 6860793]
- [54]. Poh S, Lin JB, Panitch A. Release of Anti-inflammatory Peptides from Thermosensitive Nanoparticles with Degradable Cross-Links Suppresses Pro-inflammatory Cytokine Production. *Biomacromolecules*. 2015; 16(4):1191–200. [PubMed: 25728363]
- [55]. Zhu Q, Chen L, Zhu P, Luan J, Mao C, Huang X, Shen J. Preparation of PNIPAM-gP (NIPAM-co-St) microspheres and their blood compatibility. *Colloids and Surfaces B: Biointerfaces*. 2013; 104:61–65. [PubMed: 23298589]
- [56]. van Wachem PB, Hogt AH, Beugeling T, Feijen J, Bantjes A, Detmers JP, van Aken WG. Adhesion of cultured human endothelial cells onto methacrylate polymers with varying surface wettability and charge. *Biomaterials*. 1987; 8(5):323–8. [PubMed: 3676418]
- [57]. Johnson C, Galis ZS. Matrix metalloproteinase-2 and -9 differentially regulate smooth muscle cell migration and cell-mediated collagen organization. *Arterioscler Thromb Vasc Biol*. 2004; 24(1):54–60. [PubMed: 14551157]
- [58]. Lee RT, Berditchevski F, Cheng GC, Hemler ME. Integrin-mediated collagen matrix reorganization by cultured human vascular smooth muscle cells. *Circ Res*. 1995; 76(2):209–14. [PubMed: 7834831]
- [59]. Latif F, Hennebry TA. Successful revascularization of re-stenosis of lower extremity arteries with localized delivery of paclitaxel. *Catheter Cardiovasc Interv*. 2008; 72(2):294–8. [PubMed: 18655111]
- [60]. Guzman LA, Labhasetwar V, Song C, Jang Y, Lincoff AM, Levy R, Topol EJ. Local intraluminal infusion of biodegradable polymeric nanoparticles. A novel approach for prolonged drug delivery after balloon angioplasty. *Circulation*. 1996; 94(6):1441–8. [PubMed: 8823004]

- [61]. Ward BC, Kavalukas S, Brugnano J, Barbul A, Panitch A. Peptide inhibitors of MK2 show promise for inhibition of abdominal adhesions. *Journal of Surgical Research*. 2011; 169(1):e27–e36. [PubMed: 21492875]
- [62]. Muto A, Panitch A, Kim N, Park K, Komalavilas P, Brophy CM, Dardik A. Inhibition of Mitogen Activated Protein Kinase Activated Protein Kinase II with MMI-0100 reduces intimal hyperplasia ex vivo and in vivo. *Vascular pharmacology*. 2012; 56(1):47–55. [PubMed: 22024359]
- [63]. Brugnano J, McMasters J, Panitch A. Characterization of endocytic uptake of MK2-inhibitor peptides. *J Pept Sci*. 2013; 19(10):629–38. [PubMed: 24014473]

In this manuscript, we present our work on the development and characterization of a novel temperature sensitive collagen-binding nanoparticle system. We demonstrate that when bound to a collagenous matrix, the nanoparticles are able to promote endothelial migration while avoiding cellular uptake. We also show that the nanoparticles are able to reduce inflammation via the release of anti-inflammatory peptides which, when combined with its ability to inhibit platelet binding, could lead to reduced intimal hyperplasia following balloon angioplasty. The drug delivery platform presented represents a unique dual therapy biomaterial wherein the nanoparticle itself plays a crucial role in the system's overall therapeutic potential while simultaneously releasing anti-inflammatory peptides.

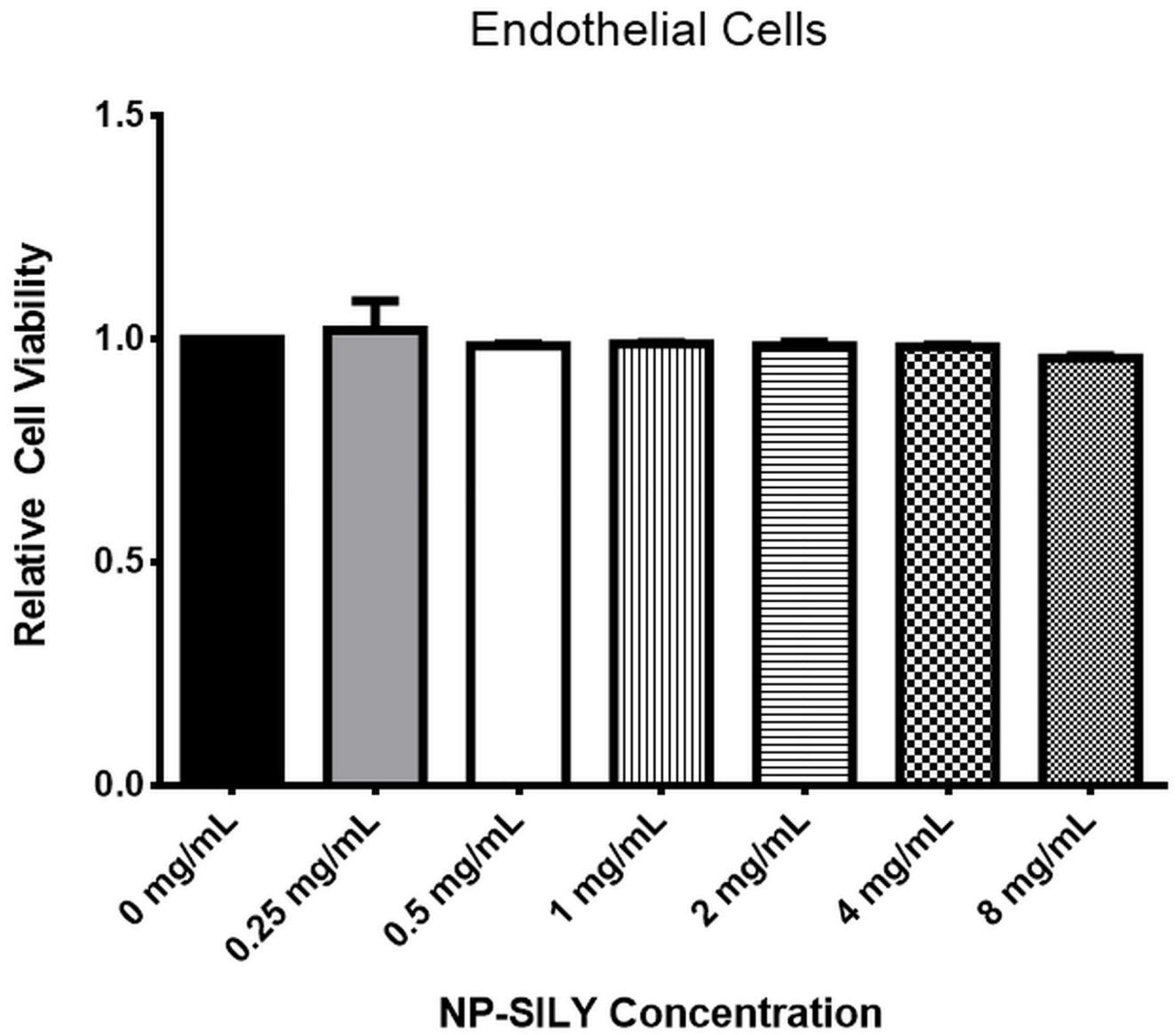
Author Manuscript

Author Manuscript

Author Manuscript

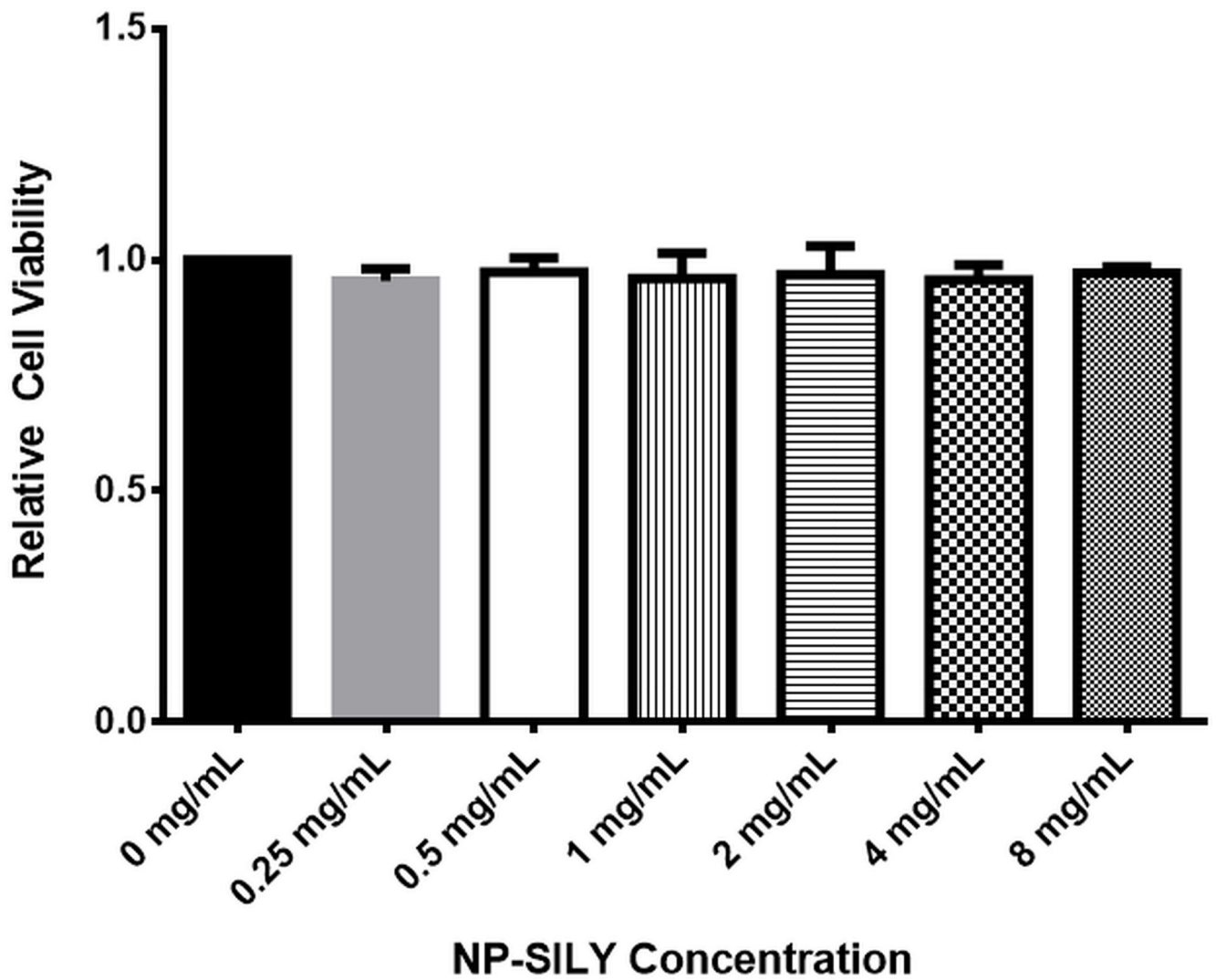
Author Manuscript

A

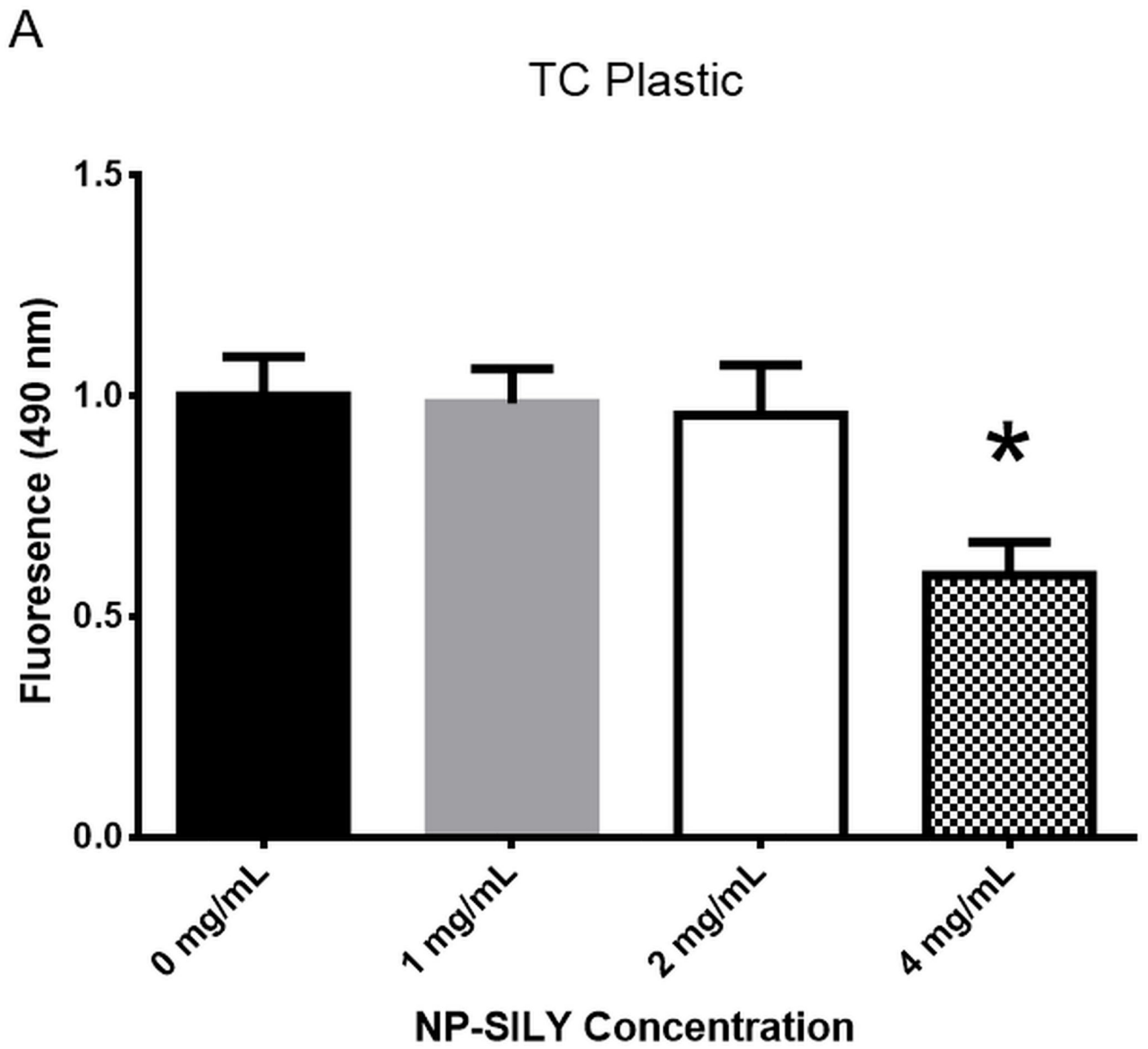


B

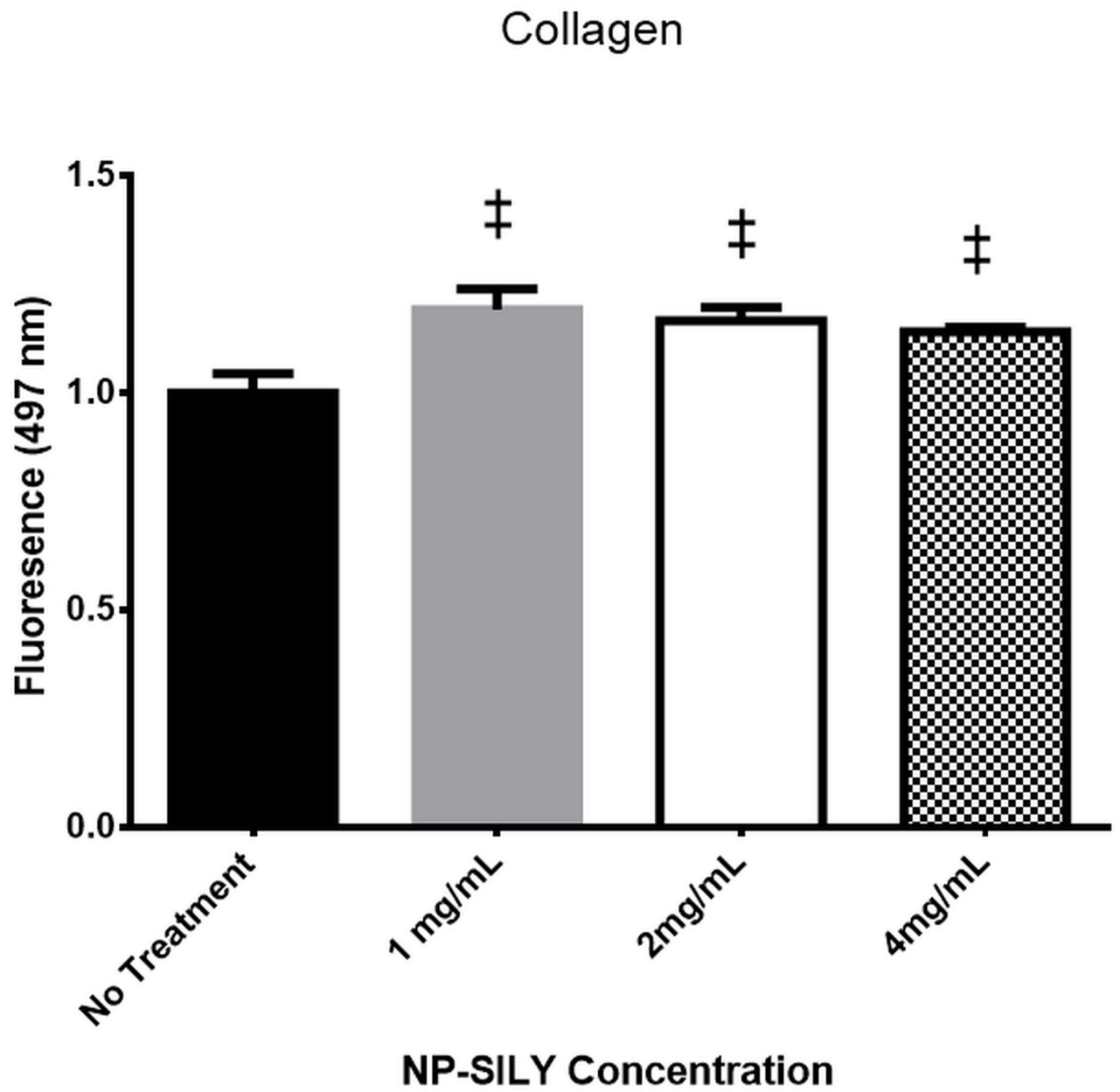
## Smooth Muscle Cells



**Figure 1.** Nanoparticle Cytotoxicity. Results of an MTT assay on Endothelial Cells (1A) and Smooth Muscle Cells (1B) treated with varying concentrations of NP-SILY over 24 hours at 37°C



B



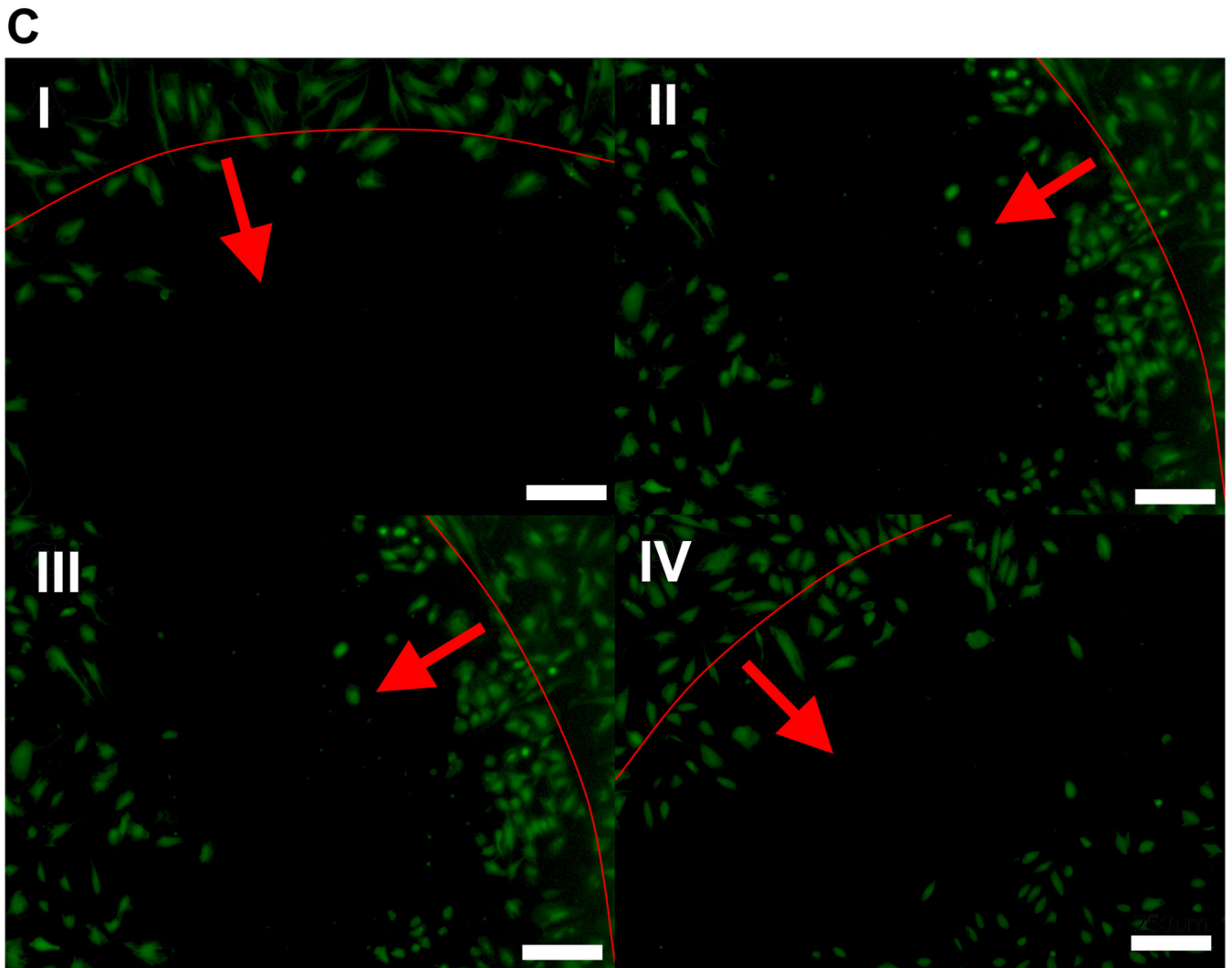
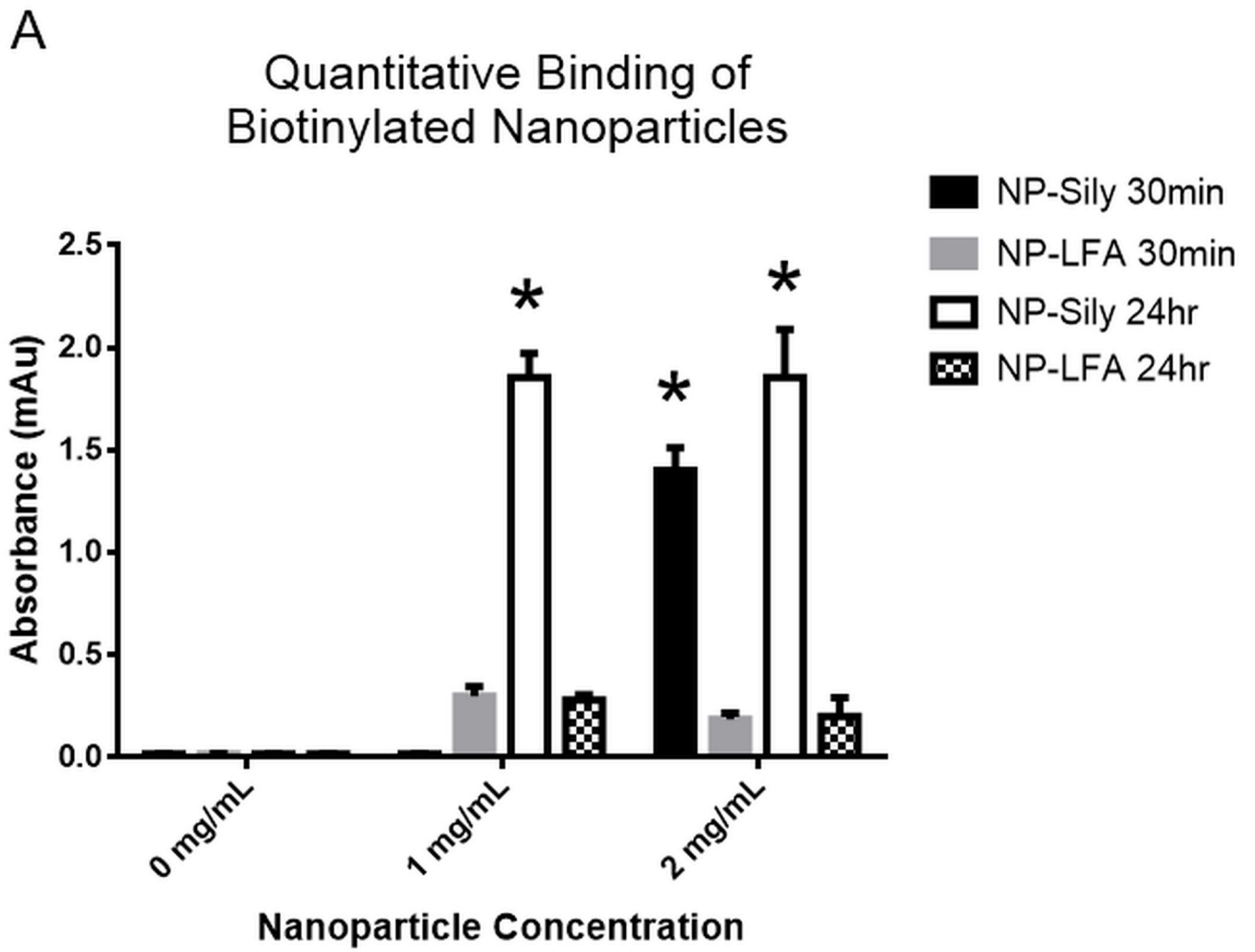
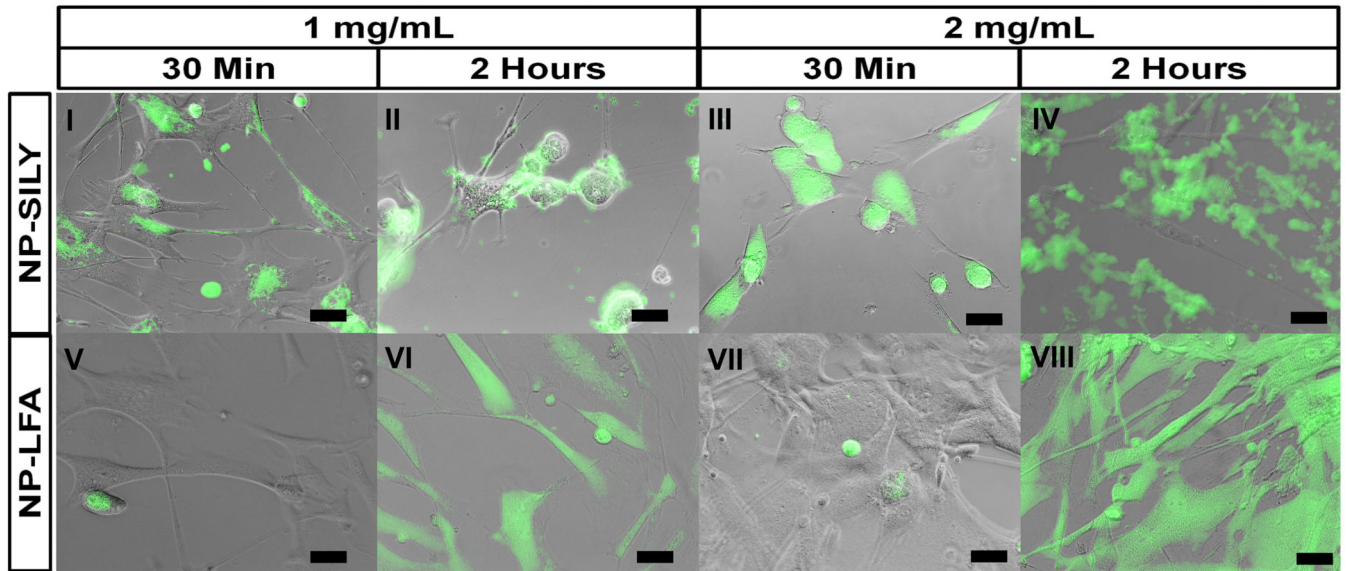


**Figure 2.** NP-SILY effect on endothelial migration. Migration of endothelial cells cultured on tissue culture plastic (2A) and a collagen-I coated surface (2B) and treated with varying concentrations of NP-SILY. \* indicates significance from all other treatments; ‡ indicates significance from untreated control. 2C: Fluorescent images of endothelial cells on a collagen surface after 24 hours of migration following treatment with NP-SILY at 0 mg/mL (I), 1 mg/mL (II), 2 mg/mL (III), and 4 mg/mL (IV), scale bar = 250  $\mu$ m. Red lines indicate edge of cell stopper that was removed prior to migration, while arrows indicate direction of cell migration.





B



C

### Binding of Fluorescent Nanoparticles

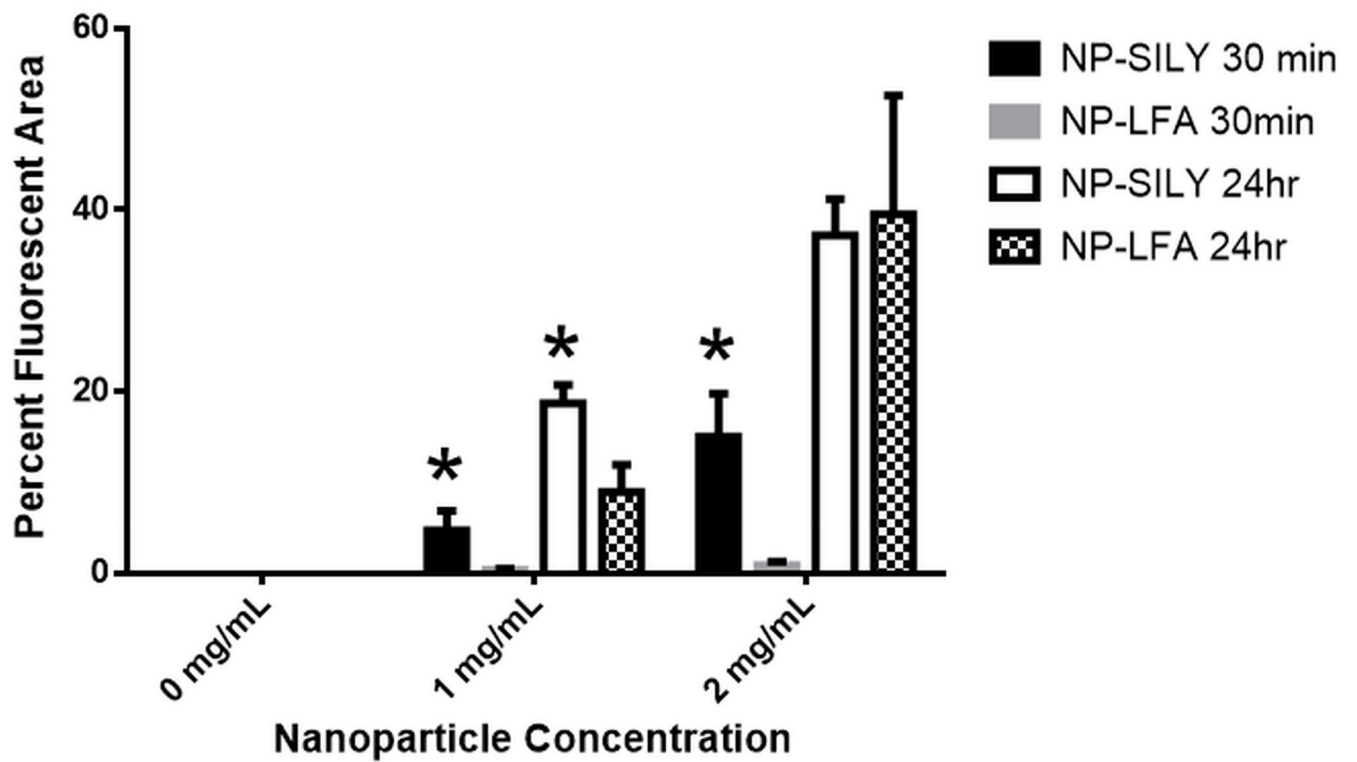
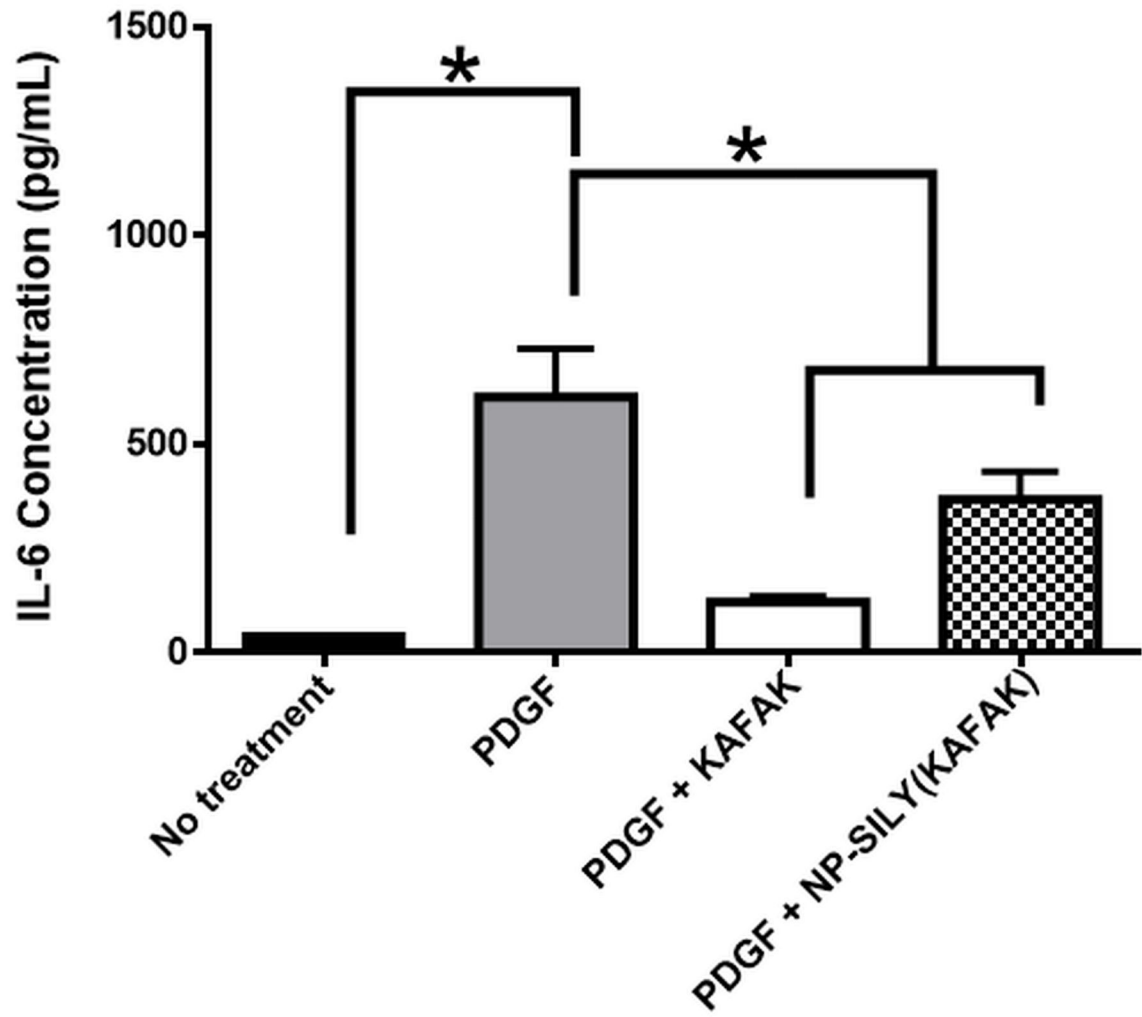


**Figure 3.**

NP-SILY binding to naturally elaborated collagen. 3A: Binding of NP-SILY biotin to collagen elaborated by cultured smooth muscle cells. Cells were treated for 30 minutes or 24 hours at 37°C. 3B: Overlay images of fluorescent NP-SILY (A,B,C,D) and NP-LFA (E,F,G,H) binding to collagen elaborated by smooth muscle cells. Cells were treated for 30 minutes (A, E, C, G) or 24 hours (B, F, D, H) at 1 mg/mL (A, B, E, F) and 2 mg/mL (C, D, G, H) of modified NPs. Scale bar = 50  $\mu$ m. 3C: Semi-quantitative image analysis of the fluorescent area of nanoparticle binding. \* indicates significance compared to LFA-modified nanoparticles at the same treatment concentration and time

A

EC Inflammation



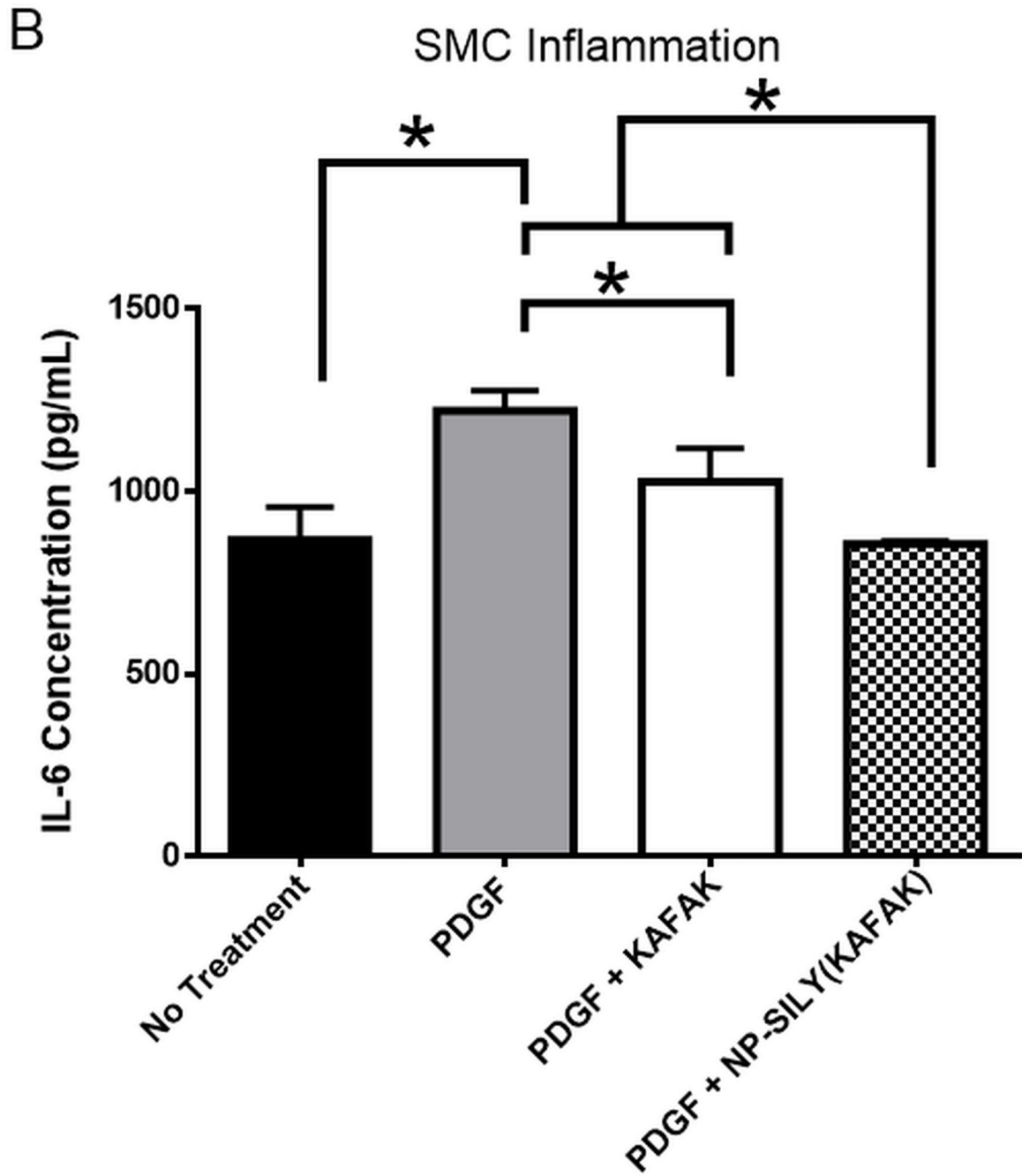


**Figure 4.** Anti-inflammatory effects of KAFAK-loaded NP-SILY. Inhibition of inflammation (measured by IL-6) in endothelial cells (4A) and smooth muscle cells (4B). Cells were treated for 24 hours at 37°C. \* represents significant differences in IL-6 levels between groups indicated by brackets.

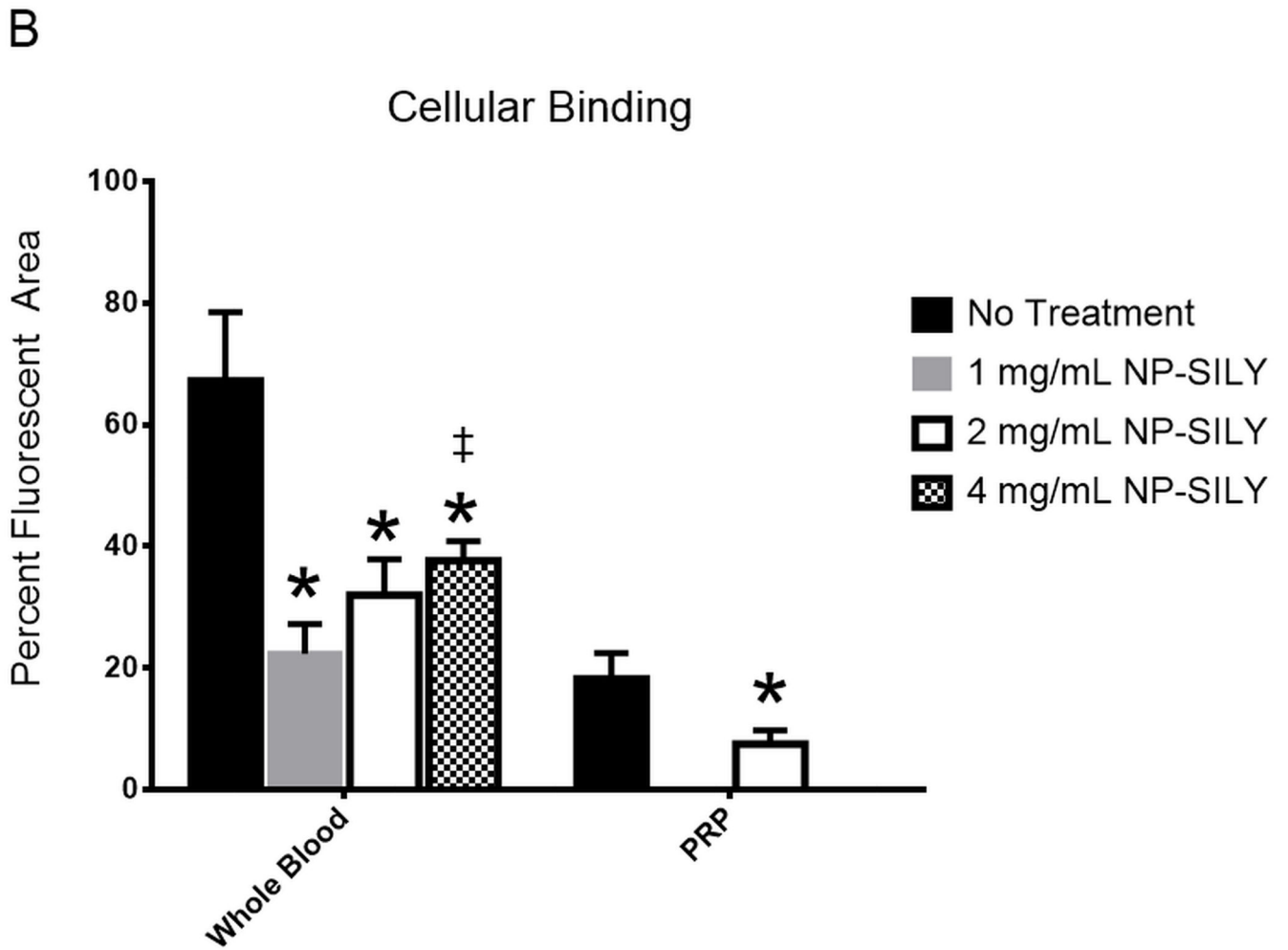
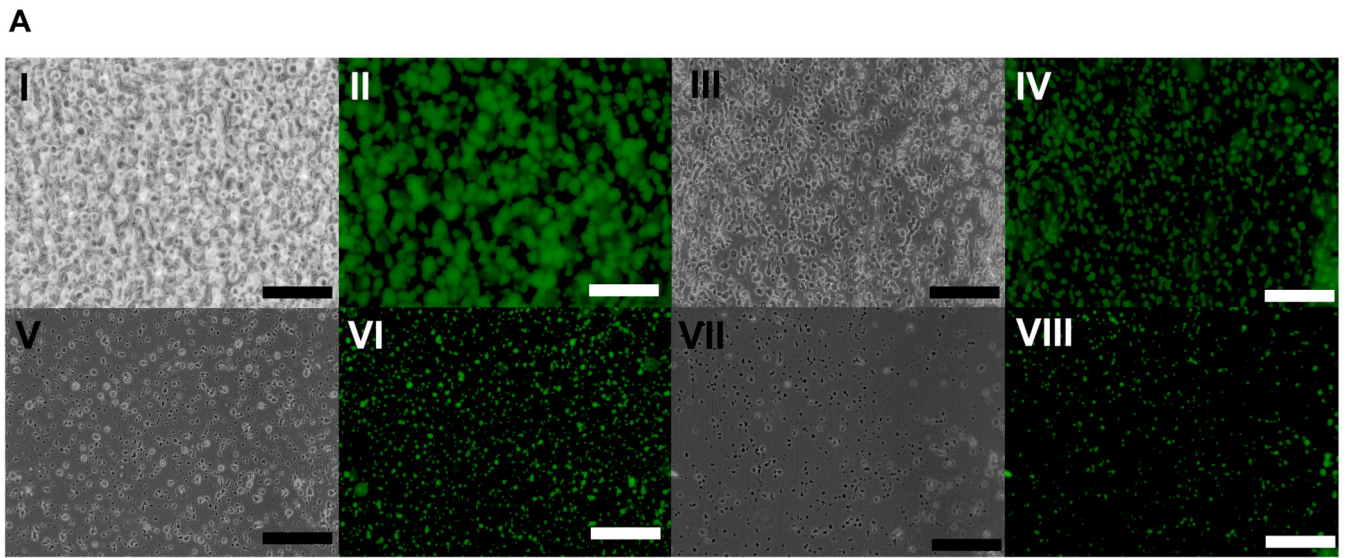


Figure 5.

NP-SILY inhibition of cellular adhesion under flow. 5A: Images of fluorescently labeled cells bound to a collagen-coated surface, (I, II, V, VI) untreated or (III, IV, VII, VIII) treated for 30 min with 2 mg/mL NP-SILY, following tangential flow of whole blood (I, II, III, IV) or platelet-rich plasma (PRP) (V, VI, VII, VIII) Scale bar = 200  $\mu\text{m}$ . 5B: Semi-quantitative image analysis of the fluorescent area of cell tracker-labeled cells shown in 5A. \* indicates significance from untreated surface; ‡ indicates significance from 1 mg/mL treatment

Author Manuscript

Author Manuscript

Author Manuscript

Author Manuscript